

Forces between elongated particles in a nematic colloid

D. Andrienko,¹ M. Tasinkevych,² P. Patrício,^{2,3} M. P. Allen,⁴ and M. M. Telo da Gama²

¹Max Planck Institute for Polymer Research, Ackermannweg 10, 55128 Mainz, Germany

²Departamento de Física da Faculdade de Ciências and Centro de Física Teórica e Computacional, Universidade de Lisboa, Avenida Professor Gama Pinto 2, P-1649-003 Lisboa Codex, Portugal

³Instituto Superior de Engenharia de Lisboa, Rua Conselheiro Emídio Navarro 1, P-1949-014 Lisboa, Portugal

⁴Center for Scientific Computing, University of Warwick, Coventry, United Kingdom

(Received 10 July 2003; published 3 November 2003)

Using molecular dynamics simulations we study the interactions between elongated colloidal particles (length to breadth ratio $\gg 1$) in a nematic host. The simulation results are compared to the results of a Landau–de Gennes elastic free energy. We find that depletion forces dominate for the sizes of the colloidal particles studied. The tangential component of the force, however, allows us to resolve the elastic contribution to the total interaction. We find that this contribution differs from the quadrupolar interaction predicted at large separations. The difference is due to the presence of nonlinear effects, namely, the change in the positions and structure of the defects and their annihilation at small separations.

DOI: 10.1103/PhysRevE.68.051702

PACS number(s): 61.30.Cz, 61.30.Jf, 61.20.Ja, 07.05.Tp

I. INTRODUCTION

Liquid crystal colloids belong to a special class of colloidal systems. Long-range orientational order of the liquid crystal molecules gives rise to additional *long-range* interactions between the colloidal particles [1,2]. The presence of defects, due to topological restrictions, controls the symmetry of this interaction that may be of dipolar or quadrupolar symmetry [3–5]. Clustering, superstructures, and new phases are immediate consequences of additional anisotropic interactions [6–8].

The long-range forces between particles of any shape can, in principle, be calculated using direct integration over the director field [9]. Ready-to-use expressions are available for spherical particles [10], two-dimensional disks [11], etc. For smaller particle-particle separations nonlinear effects from the elastic free energy come into play. Minimization of the Landau–de Gennes free energy with respect to the tensor order parameter can be used to take into account the relative position of the defects and the variation of the nematic order parameter around the colloids [11]. For even smaller separations, depletion forces, density variation, and presmectic ordering of a nematic liquid crystal near colloidal particles cannot be ignored. Then a density functional approach [12–14] or, alternatively, computer simulation techniques [15–17] can be used.

In this paper we study the interaction between elongated colloidal particles suspended in a nematic liquid crystal. The liquid crystal molecules are taken to be *homeotropically anchored*, that is, their preferred orientation is normal to the colloid surface. We compare the results of two methods: molecular dynamics simulation and minimization of the phenomenological Landau–de Gennes free energy.

It has already been shown theoretically [18] and using molecular dynamics (MD) simulation [14] that isolated small elongated particles, with homeotropic boundary conditions, minimize the free energy by orienting perpendicularly to the director. Thus, we consider the particle symmetry axes parallel to each other and perpendicular to the far field director.

In this geometry, the defect structure around a single particle has been studied in detail [19]. The configuration with two $1/2$ strength defects is preferable energetically, giving rise to a quadrupolar-type of interaction between two such particles [10]. Analytical expressions for the *long-range* forces derived from the Frank elastic free energy exist, as well as numerical studies based on the tensor order parameter formalism [11,20].

However, more detailed studies of the forces showed that the interaction between the particles is no longer quadrupolar at small separations [11], due to a change in the relative position of the defects. It was shown that the long-range repulsive interactions can become attractive for small anchoring strengths while the remaining become repulsive at all orientations for strong anchoring. As the distance between the particles decreases, their preferred relative orientation with respect to the far field nematic director changes from oblique ($\pi/4$ for the pure quadrupolar interaction) to perpendicular.

In this paper we use MD simulations to confirm this conclusion at even smaller separations, where the depletion forces play an important role. To resolve the elastic contribution to the total force we measure separately the *normal* and the *tangential* components of the force. The normal component is much larger than the tangential component and it is practically unaffected by the relative position of the defects. The tangential component, however, has a dependence on the particle separation that is qualitatively the same as that predicted by the minimization of the Landau–de Gennes free energy.

The paper is organized as follows. In Sec. II we describe the geometry, the molecular model used for MD simulation, and the technique of minimization with adaptive meshing. The director orientation, order parameter, and density maps, as well as forces between the particles, are presented in Sec. III. In Sec. IV we make some concluding remarks.

II. MOLECULAR MODEL AND SIMULATION METHODS

The geometry considered in this work is shown in Fig. 1. Two cylindrically shaped colloidal particles of radius R are

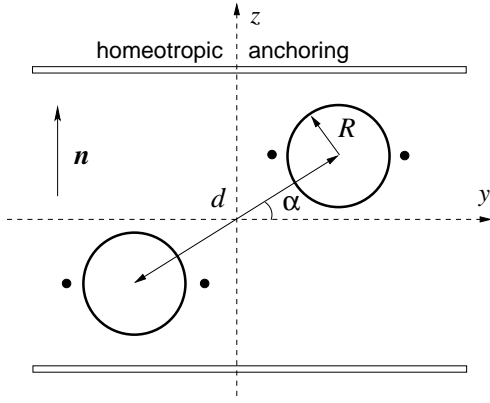


FIG. 1. Geometry (yz cross section is shown): two cylinders of radius R are immersed in a liquid crystal host. The host is modeled as a solution of Gay-Berne particles and the orientation of the director is fixed at the top and bottom walls of the simulation box ($z = \pm L_z/2$). Periodic boundary conditions are applied in the x, y directions.

immersed in a liquid crystal. The particles are separated by a distance d measured from their symmetry axes. The director orientation is fixed at the top and the bottom walls, parallel to the z axis and perpendicular to the symmetry axes of the cylinders. Boundary conditions ensure that the director \mathbf{n} far from the colloidal particles is parallel to the z axis. The rod length is considered to be infinite: in the simulations this simply means that the cylinder spans the x dimension of the periodic box.

A. MD simulation

Molecular dynamics simulations were carried out using a soft repulsive potential, describing (approximately) ellipsoidal molecules of elongation $\kappa=3$ [16]. The systems consisted of $N=8\,000$ and $64\,000$ particles (see Table I for details). A reduced temperature $k_B T/\epsilon_0=1$ was used throughout. The system size was chosen so that the number density is $\rho\sigma_0^3=0.32$, within the nematic phase for this system. Here σ_0 is a size parameter and ϵ_0 is an energy parameter (both taken to be unity).

The system is confined in the z direction, to provide uniform orientation of the director far from the particles along the z axis. The interaction of molecule i with the colloidal particle (rod) and the wall is given by a shifted Lennard-Jones repulsion potential having exactly the same form as in Refs. [16,19]. This provides homeotropic orientation with a strong anchoring of the molecules at the wall.

The radius and the length of the rod were steadily increased from zero to the desired value during 10^3 steps. Then

TABLE I. Systems studied.

Colloid radius R/σ_0	Particles N	Box size $x/\sigma_0, y/\sigma_0, z/\sigma_0$	Production (steps, 10^5)
3	8 000	10, 50, 50	10
5	64 000	20, 100, 100	5

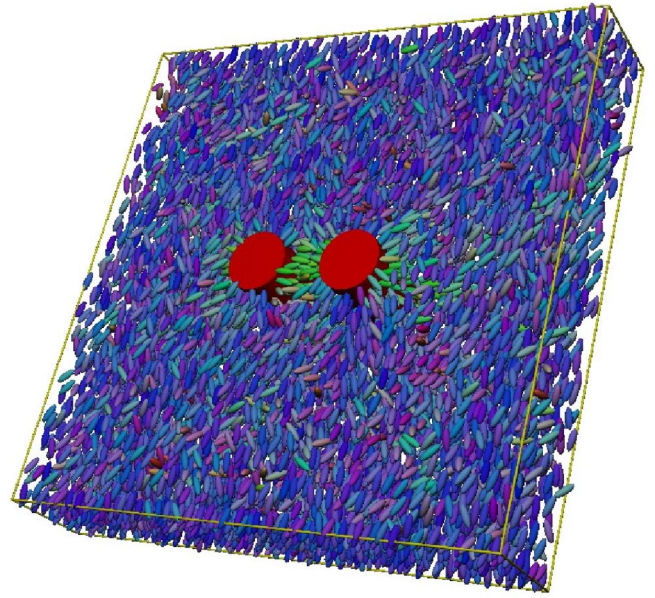


FIG. 2. (Color online) MD simulation results: snapshot of the system. Number of particles $N=8000$, colloid radius $R/\sigma_0=3$, colloid separation $d/\sigma_0=10$ and $\alpha=0$. System size $10\sigma_0 \times 50\sigma_0 \times 50\sigma_0$. Color coding emphasizes the particle orientations.

the system was equilibrated for 10^5 steps. During equilibration we scaled the velocities of the molecules to achieve $k_B T/\epsilon_0=1$. An equilibrated snapshot of the system is shown in Fig. 2.

The production run for every angle α was 10^6 steps. The force \mathbf{F} on the rod was calculated using the repulsive force f_i from the rod on the particle i :

$$\mathbf{F} = - \sum_{i=1}^N f_i. \quad (1)$$

The local tensor order parameter $\mathbf{Q}(\mathbf{r})$ was calculated as

$$Q_{\alpha\beta}(z_i, y_j) = \frac{1}{n_{\{i,j\}}} \sum_{k=1}^{n_{\{i,j\}}} \left\{ \frac{3}{2} \langle u_{k\alpha} u_{k\beta} \rangle - \frac{1}{2} \delta_{\alpha\beta} \right\}, \quad (2)$$

where there are $n_{\{i,j\}}$ molecules present in each bin $\{i,j\}$, $\delta_{\alpha\beta}$ is the Kronecker delta, $\langle \dots \rangle$ denotes an ensemble average, and $\alpha, \beta = x, y, z$. Diagonalizing the $Q_{\alpha\beta}$ tensor, for each bin, gives three eigenvalues Q_1, Q_2 , and Q_3 , plus the three corresponding eigenvectors. The eigenvalue with the largest absolute value defines the order parameter S for each bin. The biaxiality B is calculated as the absolute value of the difference between the remaining two eigenvalues of the tensor order parameter.

B. Landau–de Gennes free energy minimization

In the framework of the continuum theory, the system can be described by the Landau–de Gennes free energy [21]

$$\mathcal{F}\{\mathbf{Q}\} = \int_{\Omega} \left[\frac{L}{2} |\nabla \mathbf{Q}|^2 + f(\mathbf{Q}) \right], \quad (3)$$

where $f(\mathbf{Q})$ is a function of the invariants of \mathbf{Q} , the symmetric tensor order parameter, and the integration extends over the sample volume. Here we adopted the one-constant approximation for the elastic free energy (decoupling of the spatial and spin rotations).

To simplify the calculations, we used a two-dimensional representation of the tensor order parameter. This representation is justified for a uniaxial nematic with the director in the yz plane. Indeed, as we will see, the MD simulation results show that the director is constrained in the yz plane. The nematic is uniaxial in the bulk and is slightly biaxial in the defect core.

In this approach it is possible to rewrite \mathbf{Q} in terms of components of the director \mathbf{n} and the scalar order parameter Q :

$$Q_{ij} = Q(n_i n_j - \frac{1}{2} \delta_{ij}). \quad (4)$$

Then the Landau–de Gennes free energy density reads

$$f(\mathbf{Q}) = -\frac{a}{2} \text{Tr} \mathbf{Q}^2 + \frac{c}{4} [\text{Tr} \mathbf{Q}^2]^2, \quad (5)$$

where a is assumed to depend linearly on the temperature, whereas the positive constant c is considered temperature independent. Note that the invariant that corresponds to the cubic term of the tensor order parameter vanishes in the two-dimensional nematic.

Within this model the liquid crystal in the nematic state has the order parameter $Q_{eq} = \sqrt{2a/c}$. The elastic constant L is related to the Frank elastic constant by $K = 4La/c$. In our calculations we used $a = 1, c = 2$ which gives $Q_{eq} = 1$.

The free energy $\mathcal{F}\{\mathbf{Q}\}$ was minimized numerically, using finite elements with adaptive meshes. The geometry used in the numerical calculation is shown schematically in Fig. 1. During minimization we used a square integration region Ω of size $40R \times 40R$, where R is the radius of the colloidal particle. The area Ω was triangulated using a BL2D subroutine [22]. The tensor order parameter \mathbf{Q} was set at all vertices of the mesh and was linearly interpolated within each triangle. Using standard numerical procedures the free energy was minimized under the constraints imposed by the boundary conditions, i.e., strong homeotropic anchoring at the particle perimeters and uniform alignment at the outer boundary.

Finally, a new adapted mesh was generated iteratively from the result of the previous minimization. The new local triangle size was determined by the free energy variation of the previous solution, ensuring a constant numerical weight for each minimization variable. The final meshes with a minimal length of $\sim 10^{-3}R$ had about 2×10^4 minimization variables.

The tangential component of the interparticle force F_τ was calculated numerically from the free energy, $F_\tau = -r^{-1} \partial \mathcal{F} / \partial \alpha$.

III. RESULTS

A. Defect structures

A typical director orientation together with the density, order parameter, and biaxiality maps are shown in Fig. 3. At

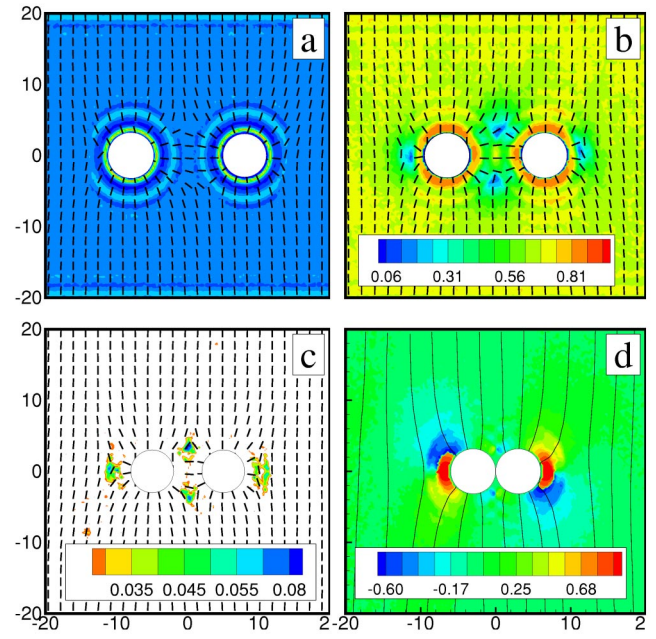


FIG. 3. (Color online) MD simulation results. Maps of (a) density at the separation $d/\sigma_0 = 16$, (b) order parameter at the separation $d/\sigma_0 = 13$ and (c) biaxiality at the separation $d/\sigma_0 = 13$. (d) shows the map of the n_y component of the director at the separation $d/\sigma_0 = 6$. The yz cross section of the system is shown. Rod radius $R = 3\sigma_0$. System size $10\sigma_0 \times 50\sigma_0 \times 50\sigma_0$. The director far from the particle is constrained along the z axis.

large separations, a pair of defect lines forms next to each particle, perpendicular to the director, as in the single colloidal particle. The director distortion vanishes very quickly in the liquid crystal bulk, and the core region extends over a few molecular lengths [19].

On reducing the separation, the positions of the defects start to change, as well as their inner structure [see Figs. 3(b,c)]. First, at relatively large separations, the plane with the defect lines tilts with respect to the particle-particle separation vector. On closer approach, the defect lines *between* the particles move away from the particles; each defect is now shared between two particles. The defect cores become more extended and lose their original, almost circular, shape. Finally, when the particles are at close contact, two out of the four defects vanish to ensure that the total topological charge in the system is zero [Fig. 3(d)].

This scenario agrees qualitatively with the results of the minimization of the Landau–de Gennes free energy [11]. In addition, in the MD simulations, we were able to observe the annihilation of the defects, which is not accessible on the length scales where the phenomenological approach is applicable. From the density map shown in Fig. 3(a) one can already see the strong influence of depletion at small separations. The order parameter map [Fig. 3(b)] illustrates the movement of the defects and the changes in the defect cores.

B. Force between the particles

Figure 4 shows typical force curves as a function of the particle-particle separation d for colloidal particles of size

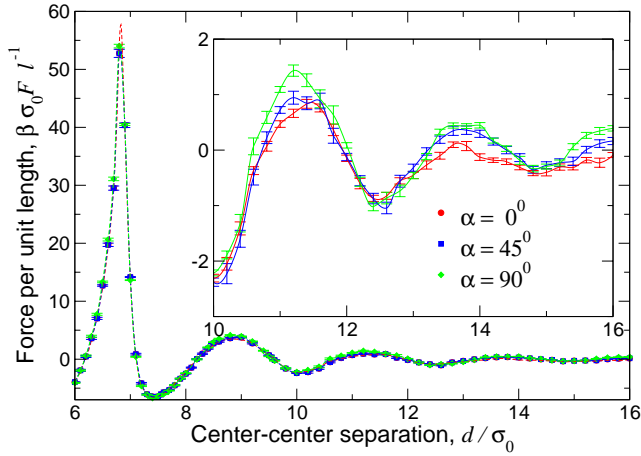


FIG. 4. (Color online) MD simulation results: components of the force parallel to the particle-particle separation vector F_{\parallel} as a function of the particle-particle separation d . Colloid radius $R/\sigma_0 = 3$.

$R/\sigma_0 = 3$. From the parallel component of the force (projection of the force on the particle-particle separation vector) one can see that the depletion forces indeed dominate; the force has oscillations due to the density modulation of the liquid crystal close to the particle surfaces (presmectic ordering). A more detailed analysis of the force curves, shown in the inset of Fig. 4, reveals that there is a small difference in the decaying tails of the force curves, which can be attributed to the elastic contribution of the order parameter field/defects around the colloidal particles to the total interparticle interaction.

To resolve the contribution of the elastic force, we plot the *tangential* component of the force (perpendicular to the particle-particle separation vector) that vanishes for isotropic systems, in Fig. 5. We first look at the situation with α

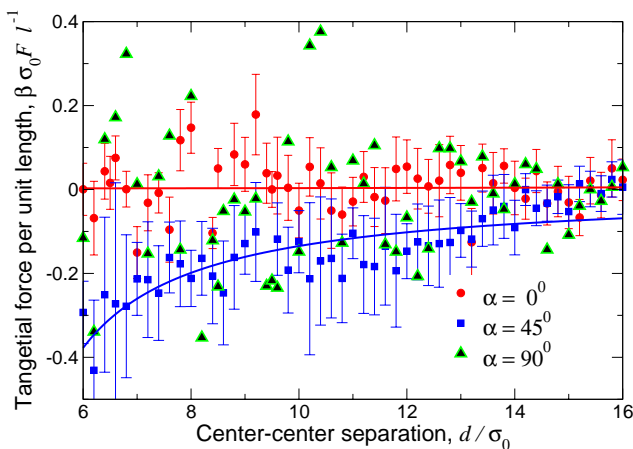


FIG. 5. (Color online) MD simulation results: component of the force perpendicular to the particle-particle separation vector F_{τ} as a function of the particle-particle separation d . Colloid radius $R/\sigma_0 = 3$. We performed a much longer run (4×10^6 steps) in order to reduce the error bars for $\alpha = 0$. Error bars for $\alpha = \pi/2$, which was run for 10^6 steps, are too large to show on the plot. Smooth curves are to guide the eye.

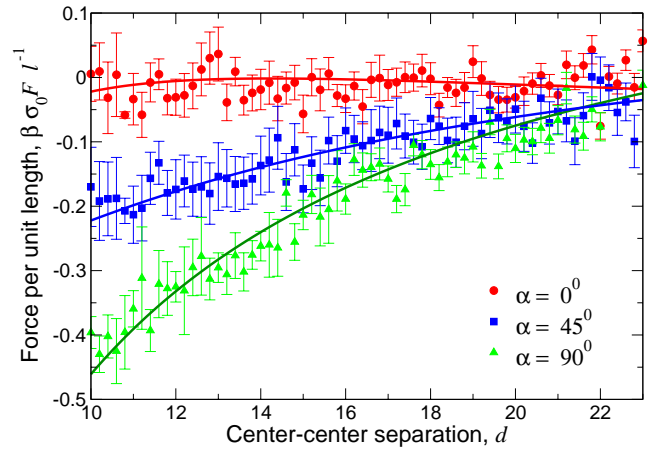


FIG. 6. (Color online) MD simulation results: component of the force perpendicular to the particle-particle separation vector F_{\perp} as a function of the particle-particle separation d . Colloid radius $R/\sigma_0 = 5$. System size $20\sigma_0 \times 100\sigma_0 \times 100\sigma_0$. Smooth curves are a guide to the eye.

$= \pi/4$. It is clear that there is a nonzero tangential component, which decays with the distance, i.e., there is a nonzero force which tends to align the particle-particle separation vector perpendicular to the director (or at some angle which is less than $\pi/4$). This is already different from the quadrupolar interaction predicted by the linear theory, where the minimum of the free energy occurs at $\alpha = \pi/4$, and agrees with the results of the Landau–de Gennes free energy minimization for small particle separations, see Ref. [11].

The situation for $\alpha = 0, \pi/2$ is somewhat different: there is a scatter in the value of the tangential component of the force, accompanied by large errors in the measurements. Analysis of the configurations suggests that this is due to a degeneracy of the defect positions. Indeed, when the particles move close to each other, the defects change their positions. The vector between the defects belonging to the same particle tilts with respect to the director. If $\alpha = 0$ or $\pi/2$, the tilt angle can be either positive or negative: both configurations are equivalent and have the same energy. However, there is a barrier between these configurations. For small particles, this barrier is of the order of $k_B T$, and the defects can switch between two equivalent configurations during the simulation run. This “drift” of the defects does not affect the parallel component of the force, but leads to the “averaging” of the tangential component to zero. In addition, this drift is slow on the time scale of a molecular simulation, and thus it leads to a large scatter in the value of the tangential force.

To overcome this problem, we studied particles with a larger radius $R = 5\sigma_0$. Correspondingly, we increased the system size to avoid self-interaction of the particles due to the periodic boundary conditions, see Table I for details. The elastic contribution to the force is larger in this case. As a consequence, the energy barrier between the two equivalent defect configurations also increases. It is thus harder for the defects to overcome this barrier that is larger than $k_B T$ for this size of the colloids. This is clearly seen from the tangential component of the force plotted in Fig. 6; the scatter of the data is smaller and there is a marked decrease with de-

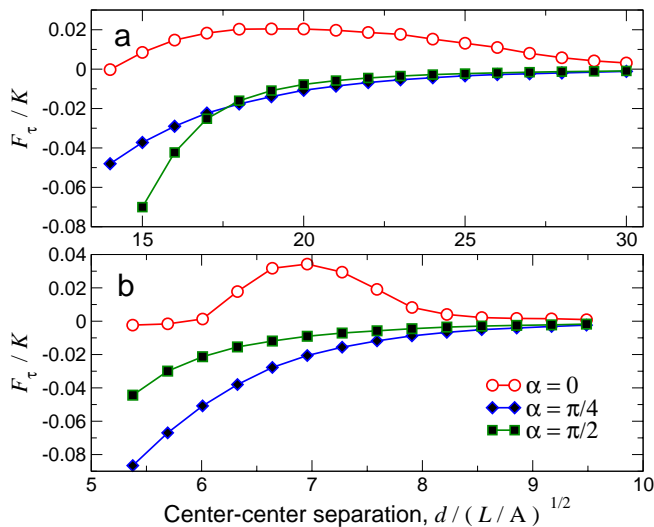


FIG. 7. (Color online) Landau–de Gennes theory: component of the force perpendicular to the vector joining the centers of the colloids as a function of the colloid separation d at three different orientations ($\alpha=0, \pi/4, \pi/2$). d is in units of the nematic correlation length $\zeta = \sqrt{L/a}$. (a) $\zeta/R=0.2$; (b) $\zeta/R=0.633$.

creasing particle–particle angle. One can also see that there is a nonzero tangential force for $\alpha = \pi/2, \pi/4$, i.e., the particles tend to align with their center-center separation vector perpendicular to the director.

Finally, we show the results of the Landau–de Gennes theory in Fig. 7. The tangential component of the force is plotted as a function of the interparticle distance d , for three different orientations of the particle–particle separation vector, $\alpha = 0, \pi/4, \pi/2$.

Comparing the results of the Landau–de Gennes theory, Fig. 7, to the MD simulation results, Fig. 6, one finds quali-

tative agreement for a value of $\zeta/R=0.2$, where $\zeta = \sqrt{L/a}$ is the nematic correlation length. To establish quantitative agreement between the two approaches, larger colloidal particles would have to be simulated (with radii of at least a few nematic correlation lengths). Simulations on such scales require a huge number of liquid crystal molecules, making them prohibitive. On the other hand, it is not possible to study very small colloidal particles using the Landau–de Gennes theory, since the theory is not valid for particles that are smaller than a few nematic correlation lengths. Consequently, the two approaches are complementary and thus a detailed quantitative comparison of the simulation and theoretical results is not meaningful.

IV. CONCLUSIONS

We used two independent techniques, molecular dynamics simulation and minimization of the Landau–de Gennes free energy, to study the interaction of two elongated colloidal particles embedded in a nematic host. Our results show that the particle–particle interaction is no longer quadrupolar at short distances due to a change in the relative position of the defects. MD simulation results also show that for small particles the depletion force dominates but contributes mostly to the interparticle radial force. The tangential contribution to the force is of elastic origin. Its dependence on the center-center separation is in qualitative agreement with the results of the free energy minimization.

ACKNOWLEDGMENTS

MD simulations used the GBMEGA program of the “Complex Fluids Consortium.” D.A. acknowledges the support of the Alexander von Humboldt Foundation. M.T. acknowledges the support of the Fundação para a Ciência e Tecnologia (FCT) through Grant No. SFRH/BPD/1599/2000.

-
- [1] P. Poulin, H. Stark, T.C. Lubensky, and D.A. Weitz, *Science* **275**, 1770 (1997).
 [2] T.C. Lubensky, D. Petey, N. Currier, and H. Stark, *Phys. Rev. E* **57**, 610 (1998).
 [3] H. Stark, *Phys. Rep.* **351**, 387 (2001).
 [4] O. Mondain-Monval, J.C. Dedieu, T. Gulik-Krzywicki, and P. Poulin, *Eur. Phys. J. E* **12**, 167 (1999).
 [5] Y. Gu and N.L. Abbott, *Phys. Rev. Lett.* **85**, 4719 (2000).
 [6] S.P. Meeker, W.C.K. Poon, J. Crain, and E.M. Terentjev, *Phys. Rev. E* **61**, R6083 (2000).
 [7] V.J. Anderson, E.M. Terentjev, S.P. Meeker, J. Crain, and W.C.K. Poon, *Eur. Phys. J.: Appl. Phys.* **4**, 11 (2001).
 [8] V.J. Anderson and E.M. Terentjev, *Eur. Phys. J. E* **4**, 21 (2001).
 [9] B.I. Lev and P.M. Tomchuk, *Phys. Rev. E* **59**, 591 (1999).
 [10] S. Ramaswamy, R. Nityananda, V. Raghunathan, and J. Prost, *Mol. Cryst. Liq. Cryst. Sci. Technol., Sect. A* **288**, 175 (1996).
 [11] M. Tasinkevych, N.M. Silvestre, P. Patricio, and M.M. Telo da Gama, *Eur. Phys. J. E* **9**, 341 (2002).
 [12] P.I.C. Teixeira, *Phys. Rev. E* **55**, 2876 (1997).
 [13] M.P. Allen, *J. Chem. Phys.* **112**, 5447 (2000).
 [14] D. Andrienko and M.P. Allen, *Phys. Rev. E* **65**, 021704 (2002).
 [15] J.L. Billeter and R.A. Pelcovits, *Phys. Rev. E* **62**, 711 (2000).
 [16] D. Andrienko, G. Germano, and M.P. Allen, *Phys. Rev. E* **63**, 041701 (2001).
 [17] E.B. Kim, R. Faller, Q. Yan, N.L. Abbott, and J.J. de Pablo, *J. Chem. Phys.* **117**, 7781 (2002).
 [18] S.V. Burylov and Y.L. Raikher, *Phys. Rev. E* **50**, 358 (1994).
 [19] D. Andrienko, M.P. Allen, G. Skacej, and S. Zumer, *Phys. Rev. E* **65**, 041702 (2002).
 [20] J. Fukuda and H. Yokoyama, *Eur. Phys. J. E* **4**, 389 (2001).
 [21] P.G. de Gennes and J. Prost, *The Physics of Liquid Crystals*, 2nd ed. (Clarendon Press, Oxford, 1995).
 [22] P.L. George and H. Borouchaki, *Delaunay Triangulation and Meshing: Application to Finite Elements* (Hermes, Paris, 1998).